Bachelor Thesis

Institut für Theoretische Physik und Astrophysik

Christian-Albrechts-Universität zu Kiel

Linear Dichroism in the Optical Absorption of Two-Dimensional Materials

Jean-Noël Varenne

15. October 2021

1. Examiner: Prof. Dr. rer. nat. Fabio Caruso

2. Examiner: Prof. Dr. rer. nat. Stefan Heinze

Contents

1 Introduction

A material is said to be dichroic when its optical absorption is dependent on the polarization of the light interacting with it. Linear and circular dichroism simply indicate the dependence on linear and circular polarization, respectively. Materials displaying dichroic properties are of significant interest in view of possible future applications, in particular in the field of valleytronics. A valleytronic device utilizes valleys, i.e. minima in conduction bands or maxima in valence bands, as additional electronic degrees of freedom. To be able to make such a device, it must be possible to confine charge carriers in one of the valleys, which can be achieved via valley-selective circular dichroism (VCD) [1]. This means that two valleys absorb left- and right-handed photons differently and thus enable the selective population of these band-edges. An example of a technology based on the valley degree of freedom is reported in the paper by Zhang et al. [2]. As an instance of a theoretical application, it possible to classify excitons by their valley configuration, which is mentioned in the paper by Yu et al.[3]. Materials which are known to display VCD are monolayer transition-metal dichalcogenides (TMDs).

The ability to control optical excitations by altering the light polarization has therefore opened new venues to achieve physical properties. Consequently, it may be of interest to study materials outside of the TMD group in regards to their dichroism more carefully, in particular two-dimensional semiconductors. It is in light of this that Phosphorene and monolayer Tin Selenide, both materials that have gained significant attention for their optoelectronic properties, shall be examined in the following.

This thesis investigates computationally the linear dichroism in Phosphorene and monolayer Tin Selenide on the grounds of Density Functional Theory while starting from first principles. In particular, the investigation is comprised of a band structure calculation, a calculation of the imaginary part of the dielectric function in the case of x- and y-polarization, a calculation of the corresponding linear dichroism and an analysis of the angular dependent linear dichroism. In chapter two, an overview of the necessary theoretical foundation to understand the results is given, and the results themselves are presented in chapter three.

2 Theoretical Background

In this chapter, the theoretical framework required to understand the computational results in the third section is briefly introduced. Most of the ideas presented in this chapter can be found in the book by Feliciano Giustino [4]; an appropriate citation is given otherwise.

2.1 The Many-Body Problem

Consider a system of N electrons and M nuclei, which can be regarded as the material of interest. Denote the electronic coordinates with $\mathbf{r}_i$, where $i \in \{1, .., N\}$. The nuclear atomic numbers shall be designated as Z_I and the nuclear coordinates as $\mathbf{R}_I$, where $I \in \{1, ..., M\}$. To set up the stationary Schrödinger equation for such a system, the Coulomb interaction between all the involved elements has to be taken into account, as well as their respective kinetic energies. The resulting many-body equation

$$
\begin{aligned}
\Bigg[&-\sum_i \frac{\nabla_i^2}{2} - \sum_I \frac{\nabla_I^2}{2M_I} - \sum_{i,I} \frac{Z_I}{|\mathbf{r}_i - \mathbf{R}_I|} \\
&+ \frac{1}{2}\sum_{i \neq j} \frac{1}{|\mathbf{r}_i - \mathbf{r}_j|} + \frac{1}{2}\sum_{I \neq J} \frac{Z_I Z_J}{|\mathbf{R}_I - \mathbf{R}_J|} \Bigg] \Psi = E_{\text{tot}}\Psi,
\end{aligned}
\tag{2.1}
$$

which is written here in Hartree units, is in the case of real systems for all practical purposes unsolvable; the storage requirements for the solution would be far greater than what is currently available on earth. It is therefore necessary to introduce some sort of approximation to acquire a useful quantitative description of the many-body problem. Fortunately, it is possible to perform a series of simplifications to generate an easier to handle set of equations, the Kohn-Sham equations, whose solutions are the core element behind the computational results in chapter three. However, it is important to mention that the following approach is a heuristic one and is only presented to formulate and give a qualitative understanding of the these equations. The rigorous justification behind this set of expressions as well as its limitations in describing the many-body system will be discussed in section 2.2.

2.1.1 Hartree-Fock Equations

The materials of interest are solids, and their firm build implies that the associated nuclei are expected to be mostly static. This means that in (2.1) the masses M_I are set to infinity, which is referred to as the clamped nuclei approximation. The nuclear coordinates $\mathbf{R}_I$ can therefore be regarded as external parameters and the interaction term between the nuclei as a constant energy shift. The many-body Hamiltonian then simplifies to

$$\hat{H}(\mathbf{r}_1,...,\mathbf{r}_N) = -\sum_i \frac{\nabla_i^2}{2} + \sum_i v_{\mathrm{n}}(\mathbf{r}_i) + \frac{1}{2}\sum_{i \neq j} \frac{1}{|\mathbf{r}_i - \mathbf{r}_j|}. \tag{2.2}$$

The first term in the brakets is responsible for the kinetic energy of the electrons, the second potential contains the term

$$v_{\mathrm{n}}(\mathbf{r}) = -\sum_I \frac{Z_I}{|\mathbf{r} - \mathbf{R}_I|}, \tag{2.3}$$

which is the Coulomb potential of the nuclei experienced by the electrons, and the third term represents the Coulomb repulsion between the electrons. Let's ignore the spin for simplicity and regard the electrons as being independent of each other, i.e. that the probability of finding an electron in one place does not depend on the position of the other electrons. In principle, this would imply leaving out the last term in (2.2) and writing the many-body wavefunction in the form of a Slater Determinant:

$$\Psi(\mathbf{r}_1,\mathbf{r}_2,\ldots,\mathbf{r}_N) = \frac{1}{\sqrt{N!}} \begin{vmatrix} \psi_1(\mathbf{r}_1) & \psi_2(\mathbf{r}_1) & \cdots & \psi_N(\mathbf{r}_1) \\ \psi_1(\mathbf{r}_2) & \psi_2(\mathbf{r}_2) & \cdots & \psi_N(\mathbf{r}_2) \\ \vdots & \vdots & \ddots & \vdots \\ \psi_1(\mathbf{r}_N) & \psi_2(\mathbf{r}_N) & \cdots & \psi_N(\mathbf{r}_N) \end{vmatrix}, \tag{2.4}$$

where each electron is described by a single-particle wavefunction $\{\psi_i\}_{i \in \{1,...,N\}}$ and Pauli's exclusion principle is satisfied. The states ψ_i would then be obtained from the single-particle Schrödinger equations

$$\left[-\frac{1}{2}\nabla^2 + v_{\mathrm{n}}(\mathbf{r}) \right] \psi_i(\mathbf{r}) = \varepsilon_i \psi_i(\mathbf{r}), \tag{2.5}$$

and the solution would be thus considerably more accessible than in the case of (2.1). It may be therefore of interest to keep the form (2.4) and apply it to (2.2) as an approximation. By minimizing the expected value of (2.2) in the state (2.4), i.e. the total energy, with respect to all possible choices of orbitals ψ_i, and requiring the orbitals to be orthonormal, the best possible approximation of the many-body wave function as a Slater Determinant is obtained. This is the so-called Hartree-Fock method which leads to the Hartree-Fock equations:

$$\left[-\frac{\nabla^2}{2} + v_{\mathrm{n}}(\mathbf{r}) + v_{\mathrm{H}}(\mathbf{r}) \right] \psi_i(\mathbf{r}) + \int d\mathbf{r}' v_{\mathrm{X}}(\mathbf{r},\mathbf{r}') \psi_i(\mathbf{r}') = \varepsilon_i \psi_i(\mathbf{r}). \tag{2.6}$$

The first additional potential, named the Hartree potential, is given by

$$v_{\mathrm{H}}(\mathrm{r}) = \sum_i \int \frac{|\psi_i(\mathbf{r})|^2}{|\mathbf{r} - \mathbf{r}'|} d\mathbf{r}'. \tag{2.7}$$

The following physical meaning may be attributed to it. If the electrons are regarded as independent of each other, the total electron charge density is the sum of the individual charge densities:

$$n(\mathbf{r}) = \sum_i |\psi_i(\mathbf{r})|^2. \tag{2.8}$$

In this case, the potential energy experienced by an electron in the electrostatic field generated by $n(\mathbf{r})$ is exactly $V_{\mathrm{H}}(\mathbf{r})$, since $V_{\mathrm{H}}(\mathbf{r})$ is the solution to the Poisson's equation describing this field:

$$\Delta v_{\mathrm{H}}(\mathrm{r}) = -4\pi n(\mathbf{r}). \tag{2.9}$$

The second potential, the exchange potential

$$v_X(\mathbf{r}, \mathbf{r}') = -\sum_j \frac{\psi_j^*(\mathbf{r}')\psi_j(\mathbf{r})}{|\mathbf{r} - \mathbf{r}'|} \tag{2.10}$$

arises from the exclusion principle and physically prevents two electrons from having the same state.

2.1.2 Kohn-Sham Equations

The Hartree-Fock equations are based on the independent particle approximation and therefore do not exactly describe the many-body system. However, the idea of simplifying the many-body problem by using a framework of non-interacting particles is attractive, since it enables the calculation of a solution through iterative means. It may be thus tempting at this point to add yet another potential to each electron that takes care of the remaining physics not incorporated into the Hartree-Fock equations. The electrons can then be thought of as each experiencing a number of potentials, which are either electrostatical or quantum mechanical in nature. Instead of having a $3N$-dimensional many-body differential equation as in (2.1), one is left with the following set of N three-dimensional single particle equations

$$\left[-\frac{\nabla^2}{2} + v_{\mathrm{n}}(\mathbf{r}) + v_{\mathrm{H}}(\mathbf{r}) + v_{xc}(\mathbf{r}) \right] \psi_i(\mathbf{r}) = \varepsilon_i \psi_i(\mathbf{r}), \tag{2.11}$$

named Kohn-Sham-equations. They implicitly include the correlation potential v_c, for which a general analytical expression doesn't exist. The potential v_c takes care of the fact that the movement of an electron is influenced by the presence of all the other electrons. The exchange potential is non-local, i.e. it is evaluated by an integral over the additional variable

$\mathbf{r}'$, and is usually replaced by the simpler local exchange potential V_x, which leads to the term $v_{xc} = v_x + v_c$ incorporated in (2.11). It may be worthwhile to emphasize here that v_H and v_{xc} both stem from the Coulomb repulsion between the electrons. In the future, the wave-functions ψ_i will be referred to as Kohn-Sham-states and their respective eigenvalues ε_i as Kohn-Sham-energies. The calculation of these physical quantities is the subject of the next section.

2.2 Density Functional Theory

In the previous section, the Kohn-Sham equations (2.11) are introduced heuristically as a simplification of the many-body equation (2.1). In this section, a rigorous approach to this simplification is given as well as a method to calculate the corresponding eigenstates and eigenvalues. To achieve this, Density Functional Theory (DFT) is used. Lastly, the Kohn-Sham equations are adapted to the case of crystalline solids.

2.2.1 Hohenberg-Kohn Theorem

Density functional theory is an exact theory of many-body systems, whose core assertions are the two Hohenberg-Kohn theorems [5]. The first theorem states that for any system of interacting particles in an external potential $V_\mathrm{ext}(\mathbf{r})$, the potential V_ext is uniquely determined, except for a constant, by the ground state particle density $n_0(\mathbf{r})$. The second theorem states that a universal functional for the energy $E[n]$ in terms of the density $n(\mathbf{r})$ can be defined, valid for any external potential $V_\mathrm{ext}(\mathbf{r})$. For any particular $V_\mathrm{ext}(\mathbf{r})$, the exact ground state energy of the system is the golbal minimum value of $E[n]$ and the ground state density $n_0(\mathbf{r})$ is the density that satisfies

$$\left. \frac{\delta E[n]}{\delta n} \right|_{n_0} = 0. \tag{2.12}$$

If the functional $E[n]$ is accessible, it is therefore possible, in principle, to determine the exact ground state density $n_0(\mathbf{r})$ and thus all properties of the system according to theorem two, since the Hamiltonian of the system is fully determined by $V_\mathrm{ext}(\mathbf{r})$.

2.2.2 The Kohn-Sham Ansatz

To obtain an expression for $E[n]$, a shorthand notation for the many-body Hamiltonian in the spirit of (2.2) is introduced:

$$\hat{H} = \hat{T} + \hat{V}_{\mathrm{n}} + \hat{V}_{ee}, \tag{2.13}$$

$$\hat{T} = -\sum_i \frac{\nabla_i^2}{2}, \tag{2.14}$$

$$\hat{V}_{\mathrm{n}} = -\sum_i v_{\mathrm{n}}(\mathbf{r}_i), \tag{2.15}$$

$$\hat{V}_{\mathrm{ee}} = \frac{1}{2} \sum_{i \neq j} \frac{1}{|\mathbf{r}_i - \mathbf{r}_j|}. \tag{2.16}$$

The total energy is obtained through the expected value of (2.13):

$$E[n] = E_{\mathrm{ext}}[n] + T[n] + U[n], \tag{2.17}$$

$$E_{\mathrm{ext}}[n] \equiv \langle\Psi|\, \hat{V}_{\mathrm{n}} \,|\Psi\rangle, \tag{2.18}$$

$$T[n] \equiv \langle\Psi|\, \hat{T} \,|\Psi\rangle, \tag{2.19}$$

$$U[n] \equiv \langle\Psi|\, \hat{V}_{\mathrm{ee}} \,|\Psi\rangle. \tag{2.20}$$

Except for $E_{\mathrm{ext}}[n]$, the exact form of each of these functionals is not known. The idea to circumvent this is to split the kinetic energy term $T[n]$ and the electron-electron interaction term $U[n]$ into a contribution from independent electrons and a supplementary term that accounts for interacting particles:

$$T[n] = T_0[n] + \alpha[n], \tag{2.21}$$

$$U[n] = E_{\mathrm{H}}[n] + \beta[n], \tag{2.22}$$

where $\alpha[n]$ and $\beta[n]$ are the unknown additional terms. By introducing the exchange and correlation energy

$$E_{\mathrm{xc}}[n] = \alpha[n] + \beta[n], \tag{2.23}$$

the total energy functional becomes

$$E[n] = T_0[n] + E_{\mathrm{ext}}[n] + E_{\mathrm{H}}[n] + E_{\mathrm{xc}}[n] \tag{2.24}$$

The Hohenberg-Kohn variational principle (2.12) may now be applied:

$$\frac{\delta}{\delta n(\boldsymbol{r})} \left\{ E[n] - \mu \left[\int d\boldsymbol{r}'n\left(\boldsymbol{r}'\right) - N \right] \right\} = 0, \tag{2.25}$$

with μ being the chemical potential. The second term in the brackets assures that the density integrates to the total number of particles. It can then be shown that the ground state density for the non-interacting system, which is defined by (2.8) and characterized by the Kohn-Sham equations (2.11), and the ground state density of the real interacting system must both satisfy

$$\frac{\delta T_0[n]}{\delta n} + v_{\mathrm{KS}}(\mathbf{r}, [n]) = \mu, \tag{2.26}$$

where

$$v_{\mathrm{KS}}(\mathbf{r}, [n]) \equiv v_{\mathrm{H}}(\mathbf{r}, [n]) + v_n(\mathbf{r}, [n]) + v_{xc}(\mathbf{r}, [n]) \tag{2.27}$$

is the Kohn-Sham potential. The term v_{H} is precisely the Hartree potential (2.7) and the last term is the exchange and correlation potential $v_{xc}(\mathbf{r}, [n]) \equiv \frac{\delta E_{\mathrm{xc}}[n]}{\delta n}$. Equation (2.26) implies that both ground state densities must coincide. A recast of the full many-body problem introduced in the first section into an independent particle problem has thus been achieved, since it is now possible to calculate the ground state density from the Kohn-Sham equations, and therefore all properties of the system in accordance with the second Hohenberg-Kohn theorem. The non-interacting system, which is referred to as Kohn-Sham system, is described by the following Schrödinger equation

$$\hat{H}_{\mathrm{KS}} \Psi_{\mathrm{KS}} = E_{\mathrm{KS}} \Psi_{\mathrm{KS}}, \tag{2.28}$$

$$\hat{H}_{\mathrm{KS}} \equiv \sum_{i}^{N} \left[-\frac{\nabla_i^2}{2} + v_{\mathrm{KS}}(\mathbf{r}_i, [n]) \right], \tag{2.29}$$

$$\Psi_{\mathrm{KS}} = \frac{1}{\sqrt{N!}} \sum_{i_1 \ldots i_N}^{N!} (-1)^{P(i_1, \ldots, i_N)} \left[\psi_{i_1}(\boldsymbol{r}_1) \ldots \psi_{i_N}(\boldsymbol{r}_N) \right], \tag{2.30}$$

$$\left[-\frac{\nabla^2}{2} + v_{\mathrm{KS}}(\mathbf{r}, [n]) \right] \psi_i(\mathbf{r}) = \varepsilon_i \psi_i(\mathbf{r}), \tag{2.31}$$

$$E_{\mathrm{KS}} = \sum_{i}^{N} \varepsilon_i. \tag{2.32}$$

Calculating the expected value $\langle \Psi_{\mathrm{KS}} | \hat{H}_{\mathrm{KS}} | \Psi_{\mathrm{KS}} \rangle$ and comparing it to (2.24) leads to the following expression for the total energy of the many-body system:

$$E[n] = E_{\mathrm{KS}} - \int v_{\mathrm{xc}}(\boldsymbol{r}) n(\boldsymbol{r}) d\boldsymbol{r} + E_{\mathrm{xc}}[n] - E_{\mathrm{H}}[n]. \tag{2.33}$$

It is crucial to remember at this point that an explicit form of the correlation and exchange energy functional is unknown and an approximation is necessitated to be able to obtain the ground state density. More on that in the section below. Once an approximation for $E_{\mathrm{xc}}[n]$ is given, the Kohn-Sham potential (2.27) is fully determined by the density n. The Kohn-Sham equations are self-consistent, i.e. the density (2.8) calculated from the orbitals

obtained through (2.30) must coincide with the density used to determine the Kohn-Sham potential. This means that a solution for the Kohn-Sham equations may be obtained by starting from a guess for the ground state density, solving (2.30), comparing it with the final density

$$n(\mathbf{r}) = \sum_i^N |\psi_i(\mathbf{r})|^2, \tag{2.34}$$

and repeating the process until a value that is accurate enough is attained. This iterative process is used to gain the results in chapter three. It is noted that only the ground state at $T = 0\,\mathrm{K}$ is considered in the rest of this thesis.

2.2.3 Local Density Approximation

In the case of a homogeneous electron gas, an explicit expression for the exchange energy functional per unit volume exits:

$$\epsilon_x^{\mathrm{HEG}}[n(\mathbf{r})] = -\frac{3}{4}\left(\frac{3}{\pi}\right)^{\frac{1}{3}} n(\mathbf{r})^{\frac{4}{3}}. \tag{2.35}$$

For the correlation energy, however, no simple analytical expressions exists, but an accurate approximation can be acquired through stochastic numerical methods. The idea behind the local density approximation (LDA) is to treat each region $d\mathbf{r}$ of slowly varying density as a homogeneous electron gas with the local density $n(\mathbf{r})$ at the point $\mathbf{r}$. The exchange energy in such a region is then given by

$$dE_x[n(\mathbf{r})] = \epsilon_x^{\mathrm{HEG}}[n(\mathbf{r})]d\mathbf{r}, \tag{2.36}$$

and integration over the entire volume of the material leads to

$$E_x[n] = -\frac{3}{4}\left(\frac{3}{\pi}\right)^{\frac{1}{3}} \int n(\mathbf{r})^{\frac{4}{3}} d\mathbf{r}. \tag{2.37}$$

The correlation energy $E_c[n]$ obtained via numerical calculations can then be added to (2.37) to obtain $E_{xc}[n]$. The functional derivative of $E_{xc}[n]$ with respect to the density then finally gives the exchange and correlation potential functional $v_{xc}[n]$ required to solve the Kohn-Sham equations. Since the results in chapter three are all based on LDA, it may be appropriate to give some information about the accuracy of this approximation. The error of atomic and molecular energies can be expected to be lower than 0.5% and for lattice constants less than 3%. Band structure calculations can therefore be expected to have a high accuracy, but some issues exists which are addressed in the next section.

2.2.4 Application to Crystalline Solids

In the case of crystals, the Block Theorem states that the single-particle electronic wavefunctions can be expressed as the product of a function periodic in the unit cell and a plane wave

$$\psi_{i\mathbf{k}}(\mathbf{r}) = e^{i\mathbf{k}\cdot\mathbf{r}} u_{i\mathbf{k}}, \qquad (2.38)$$

$$u_{i\mathbf{k}}(\mathbf{r} + \mathbf{T}) = u_{i\mathbf{k}}(\mathbf{r}), \qquad (2.39)$$

where $\mathbf{T}$ is the lattice translation vector. Replacing ψ_i with $\psi_{i\mathbf{k}}$ in (2.30) gives the following modified Kohn-Sham equations

$$\hat{H}_{\mathbf{k}} u_{i\mathbf{k}}(\mathbf{r}) = \varepsilon_{i\mathbf{k}} u_{i\mathbf{k}}(\mathbf{r}), \qquad (2.40)$$

$$\hat{H}_{\mathbf{k}} = -\frac{1}{2}(\nabla + i\mathbf{k})^2 + v_{\mathrm{KS}}([n], \mathbf{r}). \qquad (2.41)$$

The focus is switched to the periodic function $u_{i\mathbf{k}}$ instead of the full Kohn-Sham orbital $\psi_{i\mathbf{k}}$. The periodicity of $u_{i\mathbf{k}}$ means that it is sufficient to only look for solutions inside one crystalline unit cell. Similarly, because solutions of (2.40) for $\hat{H}_{\mathbf{k}+\mathbf{G}}$ are duplicates of those for $\hat{H}_{\mathbf{k}}$, where $\mathbf{G}$ is a reciprocal lattice vector, the choice of wavevectors $\mathbf{k}$ can be restricted to the first Brillouin zone. The density (2.34) may then be rewritten as follows:

$$n(\mathbf{r}) = \sum_i^\infty \int_{\mathrm{BZ}} \frac{d\mathbf{k}}{\Omega_{\mathrm{BZ}}} f_{i\mathbf{k}} \left| u_{i\mathbf{k}}(\mathbf{r}) \right|^2, \qquad (2.42)$$

where Ω_{BZ} is the volume of the Brillouin zone and $f_{i\mathbf{k}}$ is the occupation number for the Kohn-Sham state $u_{i\mathbf{k}}$, wich can either be 1 for occupied or 0 for unoccupied states. The total Kohn-Sham energy can be rewritten in the same manner:

$$E_{\mathrm{KS}} = \sum_i^\infty \int_{\mathrm{BZ}} \frac{d\mathbf{k}}{\Omega_{\mathrm{BZ}}} f_{i\mathbf{k}} \varepsilon_{i\mathbf{k}}, \qquad (2.43)$$

which leads to the modified expression for the total energy (2.33):

$$E[n] = \sum_i^\infty \int_{\mathrm{BZ}} \frac{d\mathbf{k}}{\Omega_{\mathrm{BZ}}} f_{i\mathbf{k}} \varepsilon_{i\mathbf{k}} - \int v_{\mathrm{xc}}(\boldsymbol{r}) n(\boldsymbol{r}) d\boldsymbol{r} + E_{\mathrm{xc}}[n] - E_{\mathrm{H}}[n]. \qquad (2.44)$$

This expression can be used to show that an electron carries an energy that is approximately equal to the Kohn-Sham eigenvalue $\varepsilon_{i\mathbf{k}}$ it occupies. This establishes the link between functional theory and the band theory usually presented in solid-state physics textbooks, such as the book by Kittel [], and thus gives a physical meaning for the band structures calculated in chapter three.

There is a fairly high level of agreement between DFT and experiment. However, the calculated band gaps seem to generally underestimate the measured gaps by about 40%. It can be shown that DFT/LDA calculations cannot yield the correct quasiparticle gaps. The problem lies in the Kohn-Sham formulation of DFT.

2.3 Optical Properties

After having introduced Density Functional Theory and the Kohn-Sham equations in the previous sections, these concepts are now applied to materials exposed to electromagnetic fields. This section is mainly based on chapter 12 of the book by Grosso [6].

2.3.1 Dielectric Function

In the following derivation, the CGS system is used. The chosen material shall be described by the Kohn-Sham equations (2.30). The corresponding single particle Hamiltonian may be written as

$$\hat{H}_0 = \frac{\mathbf{p}^2}{2m_e} + v_{\mathrm{KS}}(\mathbf{r}, [n]), \tag{2.45}$$

where $\mathbf{p}$ is the momentum operator. The coupling of the Kohn-Sham electron to the electromagnetic field described by the vector potential $\mathbf{A}(\mathbf{r}, t)$ and the scalar potential $\psi(\mathbf{r}, t) = 0$ yields

$$\hat{H} = \frac{1}{2m_e} \left[\mathbf{p} + \frac{e}{c}\mathbf{A}(\mathbf{r}, t) \right]^2 + v_{\mathrm{KS}}(\mathbf{r}, [n]). \tag{2.46}$$

Let the vector potential describe a transverse electromagnetic plane wave:

$$\mathbf{A}(\mathbf{r}, t) = A_0 \boldsymbol{\pi} e^{i(\mathbf{q} \cdot \mathbf{r} - \omega t)} + A_0 \boldsymbol{\pi} e^{-i(\mathbf{q} \cdot \mathbf{r} - \omega t)}, \tag{2.47}$$

where A_0 is the real amplitude and π is the light polarization vector. By neglecting the non-linear term $\mathbf{A}^2$ in (2.46) and adopting the Coulomb gauge $\nabla \cdot \mathbf{A} = 0$, the Hamiltionian becomes

$$\hat{H} = \hat{H}_0 + \frac{eA_0}{m_e c} e^{i(\mathbf{q} \cdot \mathbf{r} - \omega t)} \boldsymbol{\pi} \cdot \mathbf{p} + \frac{eA_0}{m_e c} e^{-i(\mathbf{q} \cdot \mathbf{r} - \omega t)} \boldsymbol{\pi} \cdot \mathbf{p}. \tag{2.48}$$

Transitions between Kohn-Sham orbitals are now considered in the framework of first order time-dependent perturbation theory. These transitions result from optical absorption and emission, for which the first and second perturbative term in (2.48) are responsible, respectively. Assuming the electronic states are occupied according to the Fermi-Dirac distribution function $f(E)$, and that the transitions each involve a photon with the energy $\hbar\omega$, Fermi's

golden rule gives the following net number of transitions per unit time:

$$W(\mathbf{q}, \omega) = \frac{4\pi}{\hbar} \left(\frac{eA_0}{m_e c}\right)^2 \sum_{ij} \left|\langle \psi_j | e^{i\mathbf{q}\cdot\mathbf{r}} \boldsymbol{\pi} \cdot \mathbf{p} | \psi_i \rangle\right|^2 \delta\left(\varepsilon_j - \varepsilon_i - \hbar\omega\right) \left[f\left(\varepsilon_i\right) - f\left(\varepsilon_j\right)\right], \quad (2.49)$$

with the summation going over all the possible states. The imaginary part of the dielectric function $\varepsilon_2(\mathbf{q}, \omega)$ and $W(\mathbf{q}, \omega)$ are linked via the expression

$$\varepsilon_2(\mathbf{q}, \omega) = \frac{2\pi\hbar^2}{\omega^2} \frac{1}{V} \frac{W(\mathbf{q}, \omega)}{A_0^2}, \quad (2.50)$$

where V denotes the volume of the material, and thus

$$\varepsilon_2(\mathbf{q}, \omega) = \frac{8\pi^2 e^2}{m_e^2 \omega^2} \frac{1}{V} \sum_{ij} \left|\langle \psi_j | e^{i\mathbf{q}\cdot\mathbf{r}} \boldsymbol{\pi} \cdot \mathbf{p} | \psi_i \rangle\right|^2 \delta\left(\varepsilon_j - \varepsilon_i - \hbar\omega\right) \left[f\left(\varepsilon_i\right) - f\left(\varepsilon_j\right)\right] \quad (2.51)$$

is obtained. This result may be applied to the Bloch-orbitals introduced in section 2.2.4. Since the materials under consideration are semiconductors in their ground state, only transitions from fully occupied valence states $\psi_{v\mathbf{k}}$ to empty conduction states $\psi_{c\mathbf{k}}$ are of relevance. This means that the difference of Fermi-Dirac distributions functions in (2.51) can be left out. At the same time, the wavevector $\mathbf{q}$ can be neglected, since in typical experimental situations the wavelength of the incident radiation is much larger than the lattice parameter, and thus $\mathbf{q} \ll \mathbf{k}$. This implies that only vertical transitions, i.e. transitions where the crystal momentum $\hbar\mathbf{k}$ is conserved, are taken into account. The final expression for the imaginary part of the transverse dielectric function then becomes

$$\varepsilon_2(\omega) = \frac{8\pi^2 e^2}{m_e^2 \omega^2} \sum_{cv} \int_{\mathrm{BZ}} \frac{d\mathbf{k}}{(2\pi)^3} \left|\boldsymbol{\pi} \cdot \mathbf{M}_{cv\mathbf{k}}\right|^2 \delta\left(\varepsilon_{c\mathbf{k}} - \varepsilon_{v\mathbf{k}} - \hbar\omega\right), \quad (2.52)$$

where $\mathbf{M}_{cv\mathbf{k}}$ indicates the dipole matrix element $\langle \psi_{c\mathbf{k}} | \mathbf{p} | \psi_{v\mathbf{k}} \rangle$. The delta function in (2.52) suggests that only contributions from transitions where the difference in energy between valence and conduction states is $\hbar\omega$ are possible. It may be convenient at this point to give the relationship between $\varepsilon_2(\omega)$ and the absorption coefficient:

$$\alpha(\omega) = \frac{\omega}{cn(\omega)} \varepsilon_2(\omega) \quad (2.53)$$

with the refractive index $n(\omega)$. The onset of optical absorption thus corresponds to the smallest energy difference $\varepsilon_{c\mathbf{k}} - \varepsilon_{v\mathbf{k}}$, i.e. the direct band gap, unless the associated dipole matrix element vanishes due to the symmetry of the wavefunctions. The real part and the

imaginary part of the dielectric function are linked via the Kramers-Kronig relation:

$$\varepsilon_1(\omega) = 1 + \frac{1}{\pi}\mathcal{P}\int_{\infty}^{\infty}\frac{\varepsilon_2(\omega')}{\omega' - \omega}d\omega', \tag{2.54}$$

where $\mathcal{P}$ denotes the principal part. This property can be used to to acquire the full expression for the transverse dielectric function:

$$\varepsilon(\omega) = 1 + \frac{8\pi^2 e^2 \hbar^2}{m_e^2 \Omega N_k}\sum_{\sigma}^{\uparrow\downarrow}\sum_{nm}\sum_{\mathbf{k}}^{\text{BZ}}\frac{|\boldsymbol{\pi}\cdot\mathbf{M}_{nm\mathbf{k}}|^2}{(\varepsilon_{m\mathbf{k}}^{\sigma} - \varepsilon_{n\mathbf{k}}^{\sigma})^2}\frac{(f_{n\mathbf{k}}^{\sigma} - f_{m\mathbf{k}}^{\sigma})}{\varepsilon_{m\mathbf{k}}^{\sigma} - \varepsilon_{n\mathbf{k}}^{\sigma} - \hbar\omega - i\eta}. \tag{2.55}$$

This expression is precisely the one used for the calculations in chapter three. It involves an extra summation over the spin states σ, the volume of the unit cell Ω, the number of $\mathbf{k}$-points in the Brillouin Zone N_k, as well as the intersmear parameter η. The integral in (2.52) is replaced with a discrete sum, which is necessary for practical calculations and will be briefly discussed in Section 2.3.3. To separate (2.55) back into real and imaginary part, the following identity can be used:

$$\lim_{\eta \to 0^+}\frac{1}{x - i\eta} = \mathcal{P}\frac{1}{x} + i\pi\delta(x), \tag{2.56}$$

when $x = \varepsilon_{m\mathbf{k}}^{\sigma} - \varepsilon_{n\mathbf{k}}^{\sigma}$ is inserted. The number of valence and conduction band pairs per energy interval that can contribute to the absorption is given by the so-called joint density of states:

$$J(\omega) = \sum_{\sigma}\sum_{cv}\frac{1}{\Omega_{\text{BZ}}}\int\delta(\varepsilon_{c\mathbf{k}}^{\sigma} - \varepsilon_{v\mathbf{k}^{\sigma}} - \hbar\omega)d\mathbf{k}. \tag{2.57}$$

In general, the dipole matrix element $|\boldsymbol{\pi}\cdot\mathbf{M}_{cv\mathbf{k}}|$ is a smooth function of $\mathbf{k}$ over the Brillouin zone and it's average can be factorized out of the integral in 2.52. In this case, the imaginary part of the dielectric function is proportional to $J(\omega)$.

2.3.2 Linear Dichroism

The case of linearly polarized light in the xy-plane is now considered. This means that the light polarization vector can be written as

$$\boldsymbol{\pi} = \cos\theta\mathbf{x} + \sin\theta\mathbf{y}, \tag{2.58}$$

where $\theta \in [0, \pi]$ is the polar angle and $\mathbf{x}$ and $\mathbf{y}$ the unit vectors in direction of the x and y axes, respectively. The shorthand notation for the operator

$$\square = \frac{8\pi^2 e^2 \hbar^2}{m_e^2 \Omega N_k} \sum_\sigma^{\uparrow\downarrow} \sum_{nm} \sum_{\mathbf{k}}^{\text{BZ}} \frac{f_{n\mathbf{k}}^\sigma - f_{m\mathbf{k}}^\sigma}{(\varepsilon_{m\mathbf{k}}^\sigma - \varepsilon_{n\mathbf{k}}^\sigma)^2} \frac{1}{\varepsilon_{m\mathbf{k}}^\sigma - \varepsilon_{n\mathbf{k}}^\sigma - \hbar\omega - i\eta} \tag{2.59}$$

is defined and the dielectric tensor

$$\varepsilon^{\alpha\beta}(\omega) = \delta_{\alpha\beta} + \frac{4\pi e^2 \hbar^2}{m_e^2 \Omega N_k} \sum_{nm\mathbf{k}\sigma} \frac{M_{nm\mathbf{k}}^\alpha M_{mn\mathbf{k}}^\beta}{(\Delta\varepsilon_{mn\mathbf{k}}^\sigma)^2} \frac{(f_{n\mathbf{k}}^\sigma - f_{m\mathbf{k}}^\sigma)}{(\Delta\varepsilon_{mn\mathbf{k}}^\sigma - \hbar\omega - i\eta)} \tag{2.60}$$

is introduced, where $\alpha, \beta \in \{x, y, z\}$ and $M_{mn\mathbf{k}}^v \equiv \mathbf{v} \cdot \mathbf{M}_{nm\mathbf{k}}$ with $\mathbf{v} \in \{\mathbf{x}, \mathbf{y}, \mathbf{z}\}$. Let $c = \cos\theta$ and $s = \sin\theta$. The product of $\boldsymbol{\pi}$ with the dipole matrix element yields

$$\begin{aligned}
|\boldsymbol{\pi} \cdot \mathbf{M}_{nm\mathbf{k}}|^2 &= |cM_{mn\mathbf{k}}^x + sM_{mn\mathbf{k}}^y|^2 \\
&= (cM_{mn\mathbf{k}}^x + sM_{mn\mathbf{k}}^y)(M_{mn\mathbf{k}}^x + sM_{mn\mathbf{k}}^y)^* \\
&= |c|^2 |cM_{mn\mathbf{k}}^x|^2 + |s|^2 |M_{mn\mathbf{k}}^y|^2 + cs \left[M_{mn\mathbf{k}}^x M_{mn\mathbf{k}}^y + (M_{mn\mathbf{k}}^x M_{mn\mathbf{k}}^y)^* \right] \\
&= |c|^2 |cM_{mn\mathbf{k}}^x|^2 + |s|^2 |M_{mn\mathbf{k}}^y|^2 + 2cs\text{Re}\left(M_{mn\mathbf{k}}^x M_{mn\mathbf{k}}^y \right).
\end{aligned} \tag{2.61}$$

The dielectric function (2.55) thus becomes

$$\begin{aligned}
\varepsilon(\omega) &= 1 + c^2 \square |M_{mn\mathbf{k}}^x|^2 + s^2 \square |M_{mn\mathbf{k}}^y|^2 + 2cs\square \, \text{Re}\left(M_{mn\mathbf{k}}^x M_{mn\mathbf{k}}^y \right) \\
&\overset{(2.60)}{=} 1 + c^2 \left[\varepsilon^{xx}(\omega) - 1 \right] + s^2 \left[\varepsilon^{yy}(\omega) - 1 \right] + 2cs\square \, \text{Re}\left(M_{mn\mathbf{k}}^x M_{mn\mathbf{k}}^y \right).
\end{aligned} \tag{2.62}$$

By using the properties $\cos^2\theta + \sin^2\theta = 1$ and $2\cos\theta\sin\theta = \sin(2\theta)$, the imaginary part of the dielectric function may therefore be written as

$$\varepsilon_2^\theta(\omega) = \cos^2\theta \, \varepsilon^{xx}(\omega) + \sin^2\theta \, \varepsilon^{yy}(\omega) + \sin(2\theta)\text{Im}\,\varepsilon_{\text{LD}}^{xy}(\omega), \tag{2.63}$$

$$\varepsilon_{\text{LD}}^{xy} \equiv \square \, \text{Re}\left(M_{mn\mathbf{k}}^x M_{mn\mathbf{k}}^y \right). \tag{2.64}$$

As a remark, the frequency dependence of $\varepsilon_{\text{LD}}^{xy}$ results from the operator (2.59). The linear dichroism (LD) is defined as the change in absorption due to the rotation of the polarization vector by ninety degrees:

$$\begin{aligned}
\mathscr{L}(\omega, \theta) &= \varepsilon_2^\theta(\omega) - \varepsilon_2^{\theta + \frac{\pi}{2}}(\omega) \\
&= \left[\cos^2\theta - \cos^2\left(\theta + \frac{\pi}{2}\right) \right] \varepsilon^{xx}(\omega) + \left[\sin^2\theta - \sin^2\left(\theta + \frac{\pi}{2}\right) \right] \varepsilon^{yy}(\omega) \\
&\quad + \left[\sin 2\theta - \sin\left(2\left(\theta + \frac{\pi}{2}\right)\right) \right] \text{Im}\,\varepsilon_{\text{LD}}^{xy}(\omega).
\end{aligned} \tag{2.65}$$

The following identities may be applied to simplify the above expression:

$$\cos\left(\theta + \frac{\pi}{2}\right) = -\sin\theta \Rightarrow \cos^2\theta - \sin^2\theta = \cos 2\theta,$$

$$\sin\left(\theta + \frac{\pi}{2}\right) = \cos\theta \Rightarrow \sin^2\theta - \cos^2\theta = -\cos 2\theta,$$

$$\sin\left(2\theta + \pi\right) = -\sin 2\theta,$$

which finally yields

$$\mathscr{L}(\omega, \theta) = \mathscr{L}_{\text{dia}}(\omega, \theta) + \mathscr{L}_{\text{off}}(\omega, \theta), \tag{2.66}$$

$$\mathscr{L}_{\text{dia}}(\omega, \theta) \equiv \cos(2\theta)\left[\varepsilon^{xx}(\omega) - \varepsilon^{yy}(\omega)\right], \tag{2.67}$$

$$\mathscr{L}_{\text{off}}(\omega, \theta) \equiv 2\sin(2\theta)\text{Im}\,\varepsilon_{\text{LD}}^{xy}(\omega). \tag{2.68}$$

The summand $\mathscr{L}_{\text{dia}}(\omega, \theta)$ is the diagonal component and $\mathscr{L}_{\text{off}}(\omega, \theta)$ is the off-diagonal component of the linear dichroism. To study the the angular dependence of $\mathscr{L}$, it may be worthwhile to consider the functional

$$\mathcal{F}[\mathscr{L}] \equiv \left|\int_{\omega_0}^{\omega_1} \mathscr{L}(\omega, \theta)d\omega\right|, \tag{2.69}$$

for which an energy range $[\hbar\omega_0, \hbar\omega_1]$ of interest is chosen. The comparison with the associated functionals $\mathcal{F}[\mathscr{L}_{\text{dia}}]$ and $\mathcal{F}[\mathscr{L}_{\text{off}}]$ may then give an insight into the influence of the diagonal and off-diagonal components on $\mathscr{L}$.

2.3.3 Computational Methodology

To obtain the linear dichroism (2.66) for a given polar angle θ, a calculation of the dielectric tensor components $\varepsilon^{xx}(\omega)$, $\varepsilon^{yy}(\omega)$ and the off-diagonal expression $\varepsilon_{\text{LD}}^{xy}(\omega)$ for a given frequency range is required. The software package used for this purpose is QUANTUM ESPRESSO []. The essential ingredients to calculate the tensor components are the Kohn-Sham states and energies, as can bee seen from (2.60). Therefore, the first step in the calculation is to solve the Kohn-Sham equations (2.40).

Once the atomic composition and the atomic coordinates are specified, a computational cell, i.e. a spatial domain where the states $\psi_i(\mathbf{r})$ are defined, is chosen to perform the calculation. Since a single particle Kohn-Sham equation is a second-order partial differential equation, two boundary conditions on the surface of the cell for each Cartesian directions must be indicated. In the case of solids, periodic boundary conditions, where the wavefunctions and their respective gradients are forced to repeat themselves outside of the computational cell, are an appropriate choice.

An approach effective with those boundary conditions is the planewave representation. To

this end, a reciprocal lattice to the computational space is introduced, along with the reciprocal lattice vector

$$\mathbf{G} = m_1 \mathbf{b}_1 + m_2 \mathbf{b}_2 + m_3 \mathbf{b}_3, \tag{2.70}$$

where m_1, m_2 and m_3 are integers and $\mathbf{b}_1$, $\mathbf{b}_2$ and $\mathbf{b}_3$ the primite vectors of the reciprocal lattice. The planewaves $e^{i\mathbf{G}\cdot\mathbf{r}}$ automatically satisfy the periodic boundary conditions. The Kohn-Sham eigenstates may thus be written as a linear combination of such waves:

$$\psi_i(\mathbf{r}) = \sum_{\mathbf{G}} c_i(\mathbf{G}) e^{i\mathbf{G}\cdot\mathbf{r}}, \tag{2.71}$$

with the planewave coefficients $c_i(\mathbf{G})$. The above expression is a Fourier expansion and the associated coefficients may be evaluated using the standard prescription for the Fourier series of a periodic function. By inserting (2.71) into the respective Kohn-sham equation, the following identity, written in Hartree units, can be obtained

$$\frac{|\mathbf{G}|^2}{2} c_i(\mathbf{G}) + \sum_{\mathbf{G}'} v_{\text{tot}}(\mathbf{G} - \mathbf{G}') c_i(\mathbf{G}') = \varepsilon_i c_i(\mathbf{G}), \tag{2.72}$$

$$v_{\text{tot}}(\mathbf{G}) \equiv \frac{1}{V_C} \int v_{\text{KS}}(\mathbf{r}) e^{-i\mathbf{G}\cdot\mathbf{r}} d\mathbf{r}, \tag{2.73}$$

where the integration is carried over the volume of the computational cell V_C. It can be seen that the unknowns in this case are the coefficients $c_i(\mathbf{G})$ instead of the Kohn-Sham states. The fraction in the first term in (2.72) is the new expression for the kinetic energy. To acquire the planewave coefficients, the sum $\sum_{\mathbf{G}}$ has to be truncated, which can be accomplished by imposing the cut-off kinetic energy

$$E_{\text{cut}} = \frac{|\mathbf{G}_{\text{max}}|^2}{2}, \tag{2.74}$$

such that only $\mathbf{G}$-vectors with $|\mathbf{G}|^2/2 \leq E_{\text{cut}}$ are included in the computation. The higher the cut-off energy, the more accurate the calculation is expected to be, since greater $\mathbf{G}$-vectors allow for greater detail in the description of the wavefunction.

As it was mentioned in Section 2.2.2, an approximation for the exchange and correlation energy has to be selected in order to get the full Kohn-Sham potential. The approximation is included in a file that also contains the so-called pseudopotential. The pseudopotential replaces the nuclear potential v_{n} and ensures that mainly Kohn-Sham valence states are calculated. This is because, to a certain approximation, only valence states partake in chemical bonding and are thus considerably more interesting than core electron states. Furthermore,

the removal of the latter leads to a substantial computational saving.

Another important aspect of the computation is the calculation of integrals, such a the one incorporated in the electron density (2.42). This can be achieved by discretizing the Brillouin zone into a mesh of $\mathbf{k}$-points. A grid of $N_1 \times N_2 \times N_3$ equally spaced points is selected for this purpose. However, not all points have to be included in the calculation. It is possible to use symmetry operations to sample a set of nonequivalent $\mathbf{k}$-points, i.e. points that cannot be represented between themselves with such operations, which makes the computation less demanding. Is $f(\mathbf{k})$ a function to be integrated over the Brillouin zone, then the discretization can be written as follows:

$$\frac{1}{\Omega_{\mathrm{BZ}}} \int f(\mathbf{k}) d\mathbf{k} \simeq \sum_{\mathbf{k}} \omega_{\mathbf{k}} f(\mathbf{k}), \tag{2.75}$$

where $\omega_{\mathbf{k}}$ is the weighting factor that takes into account the number of equivalent $\mathbf{k}$-points for a given $\mathbf{k}$-point.

3 Results
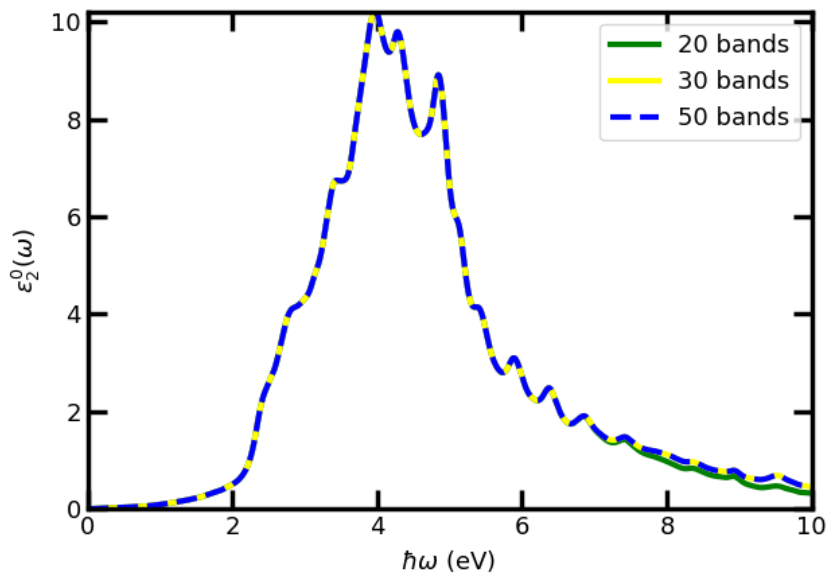
3.1 Phosphorene

3.1.1 Convergence

Figure 3.1: Comparison of the imaginary part of the dielectric function in the case of x-polarization for different band parameters.
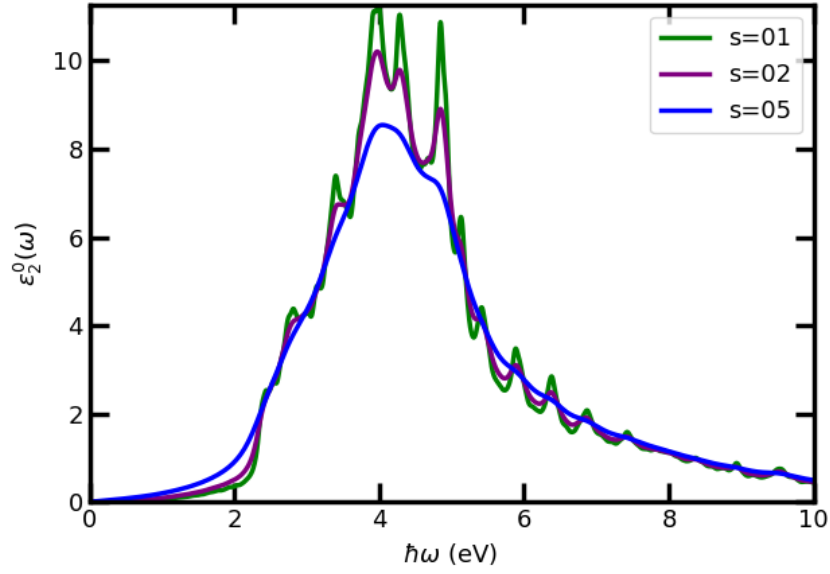
Figure 3.2: Comparison of the imaginary part of the dielectric function in the case of x-polarization for different smearing parameters.
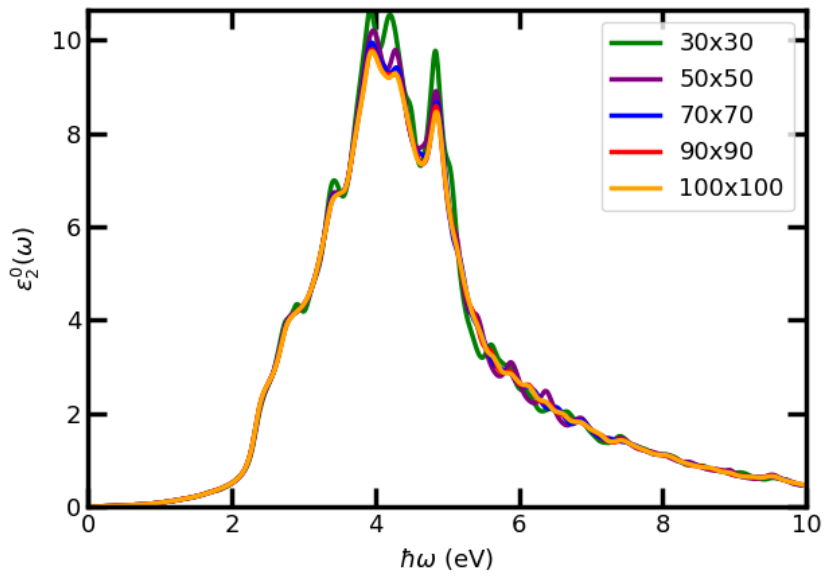

Figure 3.3: Comparison of the imaginary part of the dielectric function in the case of x-polarization for different **k**-point grid sizes.
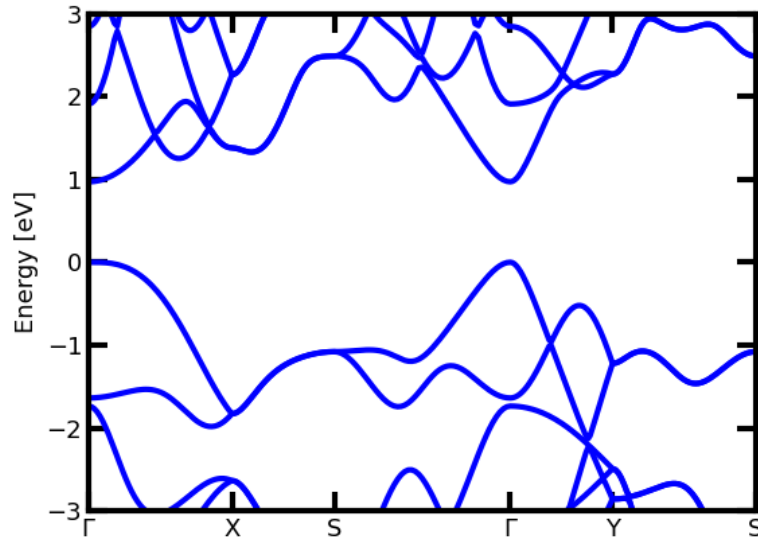
3.1.2 Band Structure

Figure 3.4: Band structure of Phosphorene for special symmetry points in the Brillouin zone.
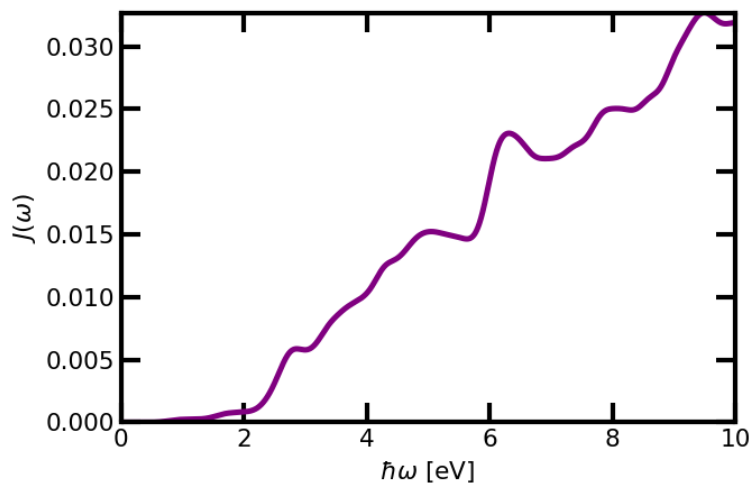
3.1.3 Dichroic Properties

Figure 3.5: Joint density of states for Phosphorene.

3.2 Tin Selenide
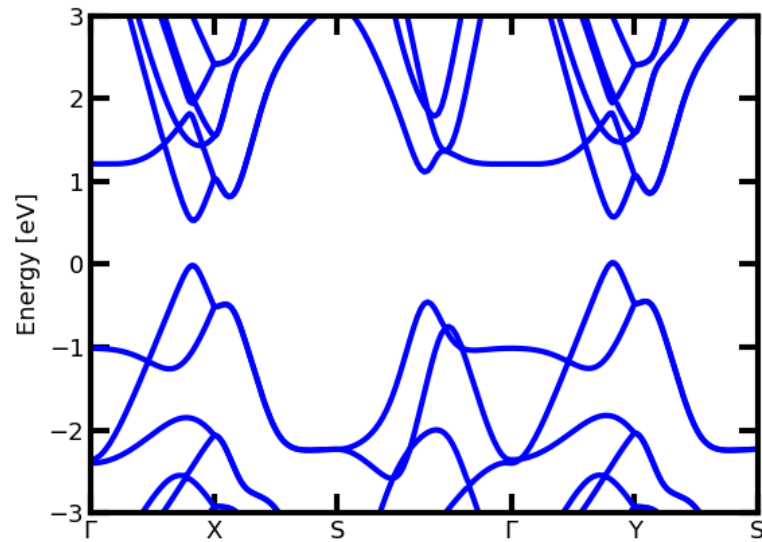
3.2.1 Convergence

3.2.2 Band Structure

Figure 3.6: Band structure of monolayer Tin Selenide for special symmetry points in the Brillouin zone.

3.2.3 Dichroic Properties

4 Conclusion and Outlook

Bibliography

[1] Kin Fai Mak et al. "Control of valley polarization in monolayer MoS2 by optical helicity". In: *nature nanotechnology* 7 (2012), pp. 494–498. DOI: 10.1038/NNANO.2012.96.

[2] Y. J. Zhang et al. "Electrically Switchable Chiral Light-Emitting Transistor". In: *SCIENCE* 344 (2014), pp. 725–728. DOI: 10.1126/science.1251329.

[3] Hongyi Yu, Xiaodong Cui, and Wang Yao. "Valley excitons in two-dimensional semiconductors". In: *Natural Science Review* 2 (2015), pp. 57–70. DOI: 10.1093/nsr/nwu078.

[4] Feliciano Giustino. *Materials Modelling Using Density Functional Theory : Properties and Predictions*. Oxford University Press, 2014. ISBN: 9780191639425. URL: https://ebookcentral.proquest.com/lib/christianalbrechts/detail.action?docID=1688422.

[5] Richard M. Martin. *Electronic Structure: Basic Theory and Practical Methods*. Cambridge University Press, 2020. ISBN: 9781108555586. DOI: https://doi.org/10.1017/9781108555586.

[6] Giuseppe Grosso and Pastori Giuseppe Parravicini. *Solid State Physics*. Elsevier Science & Technology, 2013. ISBN: 9780123850317. URL: https://ebookcentral.proquest.com/lib/christianalbrechts/detail.action?docID=1495641.

Erklärung

Ich versichere, dass ich die Bachelorarbeit selbständig und ohne unzulässige fremde Hilfe angefertigt habe und dass ich alle von anderen Autoren wörtlich übernommenen Stellen wie auch die sich an die Gedankengänge anderer Autoren eng anlehnenden Ausführungen meiner Arbeit besonders gekennzeichnet und die entsprechenden Quellen angegeben habe.

Kiel, den 15.10.2021